Illustrating Predictability for Nocturnal Tornado Events in the Southeastern United States

RYAN C. BUNKER
National Weather Center Research Experience for Undergraduates, Norman, Oklahoma
University of Oklahoma, Norman, Oklahoma

ARIEL E. COHEN
NOAA/NWS/Storm Prediction Center, Norman, Oklahoma
University of Oklahoma School of Meteorology, Norman, Oklahoma

JOHN A. HART
NOAA/NWS/Storm Prediction Center, Norman, Oklahoma

KIMBERLY E. KLOCKOW
Cooperative Institute for Mesoscale Meteorological Studies/ National Severe Storms Laboratory, Norman, Oklahoma

ALAN E. GERARD
Warning Research & Development Division/National Severe Storms Laboratory, Norman, Oklahoma

Corresponding author address: Ryan C. Bunker, University of Oklahoma School of Meteorology, 120 David L. Boren Blvd, Norman, OK 73072.
E-Mail: Ryan.C.Bunker-1@ou.edu

ABSTRACT

Nocturnal tornado events can create societal vulnerabilities when visibility is extremely limited, when people are asleep, and when people are in weak-infrastructure buildings. Understanding these high-impact events is a crucial step for forecasters to improve lead times for the public. Previous studies have assessed the ability for parameters to distinguish severe thunderstorm environments. This study uses the Statistical Severe Convective Risk Assessment Model (SSCRAM) to help assess what parameters can be linked to tornado potential in the southeast United States. This study shows that several parameters have statistically significantly different distributions between the Southeast and everywhere else in the contiguous United States, and between the coastal region subset of the Southeast and everywhere else in the contiguous United States. By adding a constraint of at least 50 knots of effective bulk shear, the predictability for tornadoes in the southeast U.S. is generally better than everywhere else. Overall, the coastal region subset offers worse predictability than everywhere else when no constraints are added. This approach to predictability can contribute to the warn-on-forecast initiatives and current-day operational forecasting.

1. Introduction

The overnight hours (03Z-12Z) are a time when society is particularly vulnerable to severe thunderstorms and tornadoes. These high-impact events are 2.5 times more likely to kill as those that occur during the daytime because of vulnerabilities such as visibility, people being asleep, and people being in weak building structures in comparison to steel or reinforced-

64 concrete buildings during the day (Ashley et al. 2008). Forecasters aim to accurately predict
65 these severe weather events in order to save lives and improve warnings. The southeast United
66 States are associated with more tornado occurrences than anywhere else in the United States
67 from November to May (Fig. 1). Galway and Pearson (1981) examined tornadoes from 1950-
68 1979 and found that 68% of all tornadoes (1040 out of 1531 tornadoes) occur within the
69 southeast United States during December to February.
70 Nocturnal tornado environments are often characterized by distinguishable
71 thermodynamic and kinematic parameters that can create many challenges for forecasters in
72 the southeastern United States owing to a higher rate of tornado occurrences than the rest of
73 the contiguous United States (Fig. 1). Tornadoes within this region are generally typified by
74 weak buoyancy and strong vertical shear (Guyer and Dean 2010), the former of which has
75 larger predictive uncertainty (e.g., Cohen et al. 2015). Weak buoyancy and strong vertical wind
76 shear are just a couple of the parameters that can be associated with convection and tornado
77 potential in the southeast United States.
78 There have been many attempts to improve forecasting techniques for tornado events
79 in recent history by incorporating numerical weather prediction models and conceptual models
80 in order to connect the gap between observations and modeling output (e.g, Schwartz et al.
81 2014, Bryan et al. 2003; Johns and Doswell 1992; Galway 1992; Burgess and Lemon 1990; Lewis
82 1989; Scofield and Purdom 1986). The result of these technological improvements has offered
83 forecasting guidance when identifying multiple individual and combined parameters that
84 distinguish environments potentially capable of producing severe thunderstorms. However,
85 small-scale processes within the planetary boundary layer associated with turbulent eddies

86 such as vertical mixing related to moisture and heat fluxes, can generate model output errors
87 (e.g, Cohen et al. 2015; Jankov and Gallus 2004).
88 Increasing the understanding of these high-impact events and the environments that
89 support such phenomena is a potentially crucial step to improving tornado predictability within
90 the southeast United States. Forecasters use an array of individual and combined parameters to
91 anticipate severe weather occurrence in order to improve forecasting for these high-impact
92 events. In this study, the southeast United States corresponds to an area depicted on a map
93 provided in Fig. 2. The coastal region, which is a subset of the general Southeast, is also
94 depicted in Fig. 2. The coastal region subset was selected as another area of focus because of
95 the extreme number of average tornado watches issued per year (Fig. 3) as well as the
96 hypothesis that this subset will not have better predictability than that of the southeast U.S. as
97 a whole when compared to the rest of the contiguous United States. These hypotheses will be
98 tested by creating conditional probability plots for different parameters and showing statistical
99 significance between distributions. In addition to focusing on these overlapping areas, this
100 study will also consider the mutually exclusive area outside of the general southeast United
101 States across the contiguous United States (subsequently referred to as “everywhere else” or
102 the like).
103 This study aims to identify a selection of parameters and combination of parameters
104 that may improve forecasting abilities for these high-impact events by using conditional
105 probabilities for numerous parameters created from the Statistical Severe Convective Risk
106 Assessment Model (Hart and Cohen 2016a). The Statistical Severe Convective Risk Assessment
107 Model (Hart and Cohen 2016a) output yields probabilities based on previous severe weather

events given different atmospheric parameters. Doswell and Schultz (2006) challenged the belief of using diagnostic parameters to accurately draw conclusions about the future state of the atmosphere. Parameters investigated in detail in the present study include the following: 0-1-km shear, 0-1-km storm-relative helicity (SRH), 100-mb mixed layer convective available potential energy (MLCAPE), 100-mb mixed layer lifted condensation level heights (MLLCL heights), effective bulk shear, effective storm-relative helicity (effective SRH), and significant tornado parameter (STP), which is defined by Thompson et al. (2012). In conjunction with this present study, the potential utility and use of SSCRAM was studied by a fellow Research Experience for Undergraduates student, David Nowicki (Nowicki 2017). The goal behind this combined study is to contribute to the warn-on-forecast program to improve warning lead times for these severe weather events (Hart and Cohen 2016a).

2. Methodology

a.) Data Collection

The probabilities used in this study are conditional upon cloud-to-ground (CG) lightning occurrence and are related to downstream tornado reports. As described by Hart and Cohen (2016a), the 40-km RUC-2/RAP grid boxes within the general southeast domain, embedded coastal domain, and the everywhere else domain are considered. SSCRAM identifies all grid boxes in each of these domains in which CG lightning occurs (Fig. 4), including several attributes such as date, time, center point of the grid box (latitude/longitude), and Bunkers et al. (2000) right-moving supercell motion to represent downstream storm trajectory within the next 2

hours as well as the environment conditions from SPC Mesoanalysis system (Bothwell et al. 2002) characteristic of the near-storm environment for that grid box.

The validity of Bunkers et al. (2000) right-moving storm motion was shown in Hart and Cohen (2016a) paper as the preferred method of calculating downstream storm trajectory based on the consistent structural patterns for conditional probability distributions for different parameters after comparing four different methods of estimating storm motion. Since the majority of tornadoes are associated with supercells, the use of Bunkers et al. (2000) storm motion is the appropriate method for high-impact weather events (Hart and Cohen 2016a). Furthermore, using Bunkers et al (2000) supercell motion does limit SSCRAM's use in distinguishing between other convective modes (Hart and Cohen 2016a).

The dataset from which these conditional probabilities arise is gathered by following Bunkers et al. (2000) storm motion 2 hours downstream from the center point of the lightning-containing grid box. Tornado reports are gathered at each subsequent hour, downstream from the center point of the lightning-containing grid box. The search radius at each subsequent hour downstream from the center point of the lightning-containing grid box is 40 km. As described in Hart and Cohen (2016a), 40-km was chosen due to the consistency of the grid length of the SPC Mesoanalysis dataset. Additionally, this radius accounts for any displacement to the storm motion downstream of the center point of the initial lightning-containing grid box. The dataset that is attained from this process links environmental parameters to tornado potential in the future.

b.) Statistical analysis procedure

Two measures of statistical analysis, with plots, are the focus in the discussion following this section corresponding to the environmental parameters described above: 1) conditional probabilities of a tornadic events, described in Hart and Cohen (2016) and 2) the statistical significance of the distributions between the southeastern U.S. and the remainder of the CONUS; and the coastal region subset and the rest of the CONUS. The conditional probabilities indicate the frequency of a tornadic event given certain atmospheric parameters associated with lightning. As an example, in this study, a conditional probability of 40% for a particular range signifies that 40% of lightning-producing thunderstorms with that parameter range go on to produce a tornado within the next 2 hours. It should be noted that the probabilities are not a forecast, but an observation based off of prior events.

A Z-Test (Kanji 2006) was used to determine whether differences between distributions are statistically significant. P-values were calculated and are overlaid on each graph to represent different distributions. A green dot represents a p-value of <0.05, which indicates that the difference between the two compared regimes for a given parameter range is statistically significantly, and a yellow dot indicates a p-value of 0.05-0.1, which indicates that the difference between the two compared regimes for a given parameter range is marginally statistically significantly different. To remain consistent with both Hart and Cohen (2016) papers, any total number of environments less than 25, will not be plotted in the figures below.

3. Results and discussion

a.) Statistical results for the southeast U.S.

Conditional probabilities of tornado events (weak or significant) for the southeast U.S are found to increase slightly with increasing 0-1-km shear, as shown in Fig. 5a. Throughout the following discussion sections, probability plots will only represent any tornado event (weak or significant) unless stated otherwise. Most of the tornado environments occur within weak-to-moderate low-level shear regimes, and the overall utility in 0-1-km shear for predicting tornadoes, is quite limited. In subsequent sections, most of the tornado environments occur within weaker regimes; however, the focus of this analysis will be examining predictability as parameters increase. Along with 0-1-km shear, 0-1-km SRH conveys the same overall pattern when it comes to predicting tornadoes as shown in Fig. 5b. The overall predictability is quite weak, while only reaching a maximum probability of 5% with a respective parameter value of 650 (m^2 s^{-2}). In contrast to 0-1-km shear and 0-1-km SRH, effective bulk shear shows a steep slope of increasing probabilities with shear values for the southeast U.S from 45 to 70 kt as shown in Fig. 4e. Along with good predictability, there is statistical significance between the southeast U.S. and everywhere else within most of this parameter range. This complements previous studies that highlight the relationship between strong shear environments and tornado occurrences within the southeast U.S. (Guyer and Dean 2010). Because southeast U.S tornado environments are typically associated with strong vertical shear and the steep slope of conditional probabilities compliments this finding, 50 kt of effective bulk shear will be used as a constraint in later sections.

Conditional probabilities of tornado events do not vary throughout the entire MLCAPE range for the southeast U.S., as shown in Fig. 5c. This suggests that low-CAPE environments during the night and early morning hours only need marginal buoyancy to maintain convective

updrafts when other environmental parameters are favorable, e.g., shear (Guyer and Dean 2010). In addition to MLCAPE, MLLCL heights show a slight increase in conditional probabilities for low-level MLLCL heights and a slight decrease for high MLLCL heights. The slight decrease in probabilities is presumed to be because of the smaller sample size characterized by these higher LCL heights.

Operational meteorologists often reference effective SRH and STP for tornado forecasting (Hart and Cohen 2016a) with analyses for these parameters in Figs 5f and 5g, respectively. The effective SRH range of 250 to 550 (m^2 s^{-2}) shows a substantial increase in probabilities from 1% to 17.5%; however, the southeast U.S. and the remainder of the CONUS follow the same distribution. Throughout the U.S., including the Southeast, good predictability is shown with high effective SRH magnitudes, reaching probability maxima at 550 (m^2 s^{-2}) of 15% and 17.5%, respectively. STP is often referenced in operational meteorology to help illustrate significant tornadoes (EF2 or greater) (Thompson et al. 2012). Lower ranges of STP (0-4) show a major increase in conditional probabilities for significant tornadoes by reaching up to 12% before slightly declining thereafter; this is presumed to be because of a smaller sample size with increasing STP values. While not shown, the signal for conditional probabilities for weak tornadoes in the southeast using STP was weak as it only reached to 6% with the same parameter range.

b.) Statistical results with a constraint of 50 kt effective bulk shear

The best predictor for tornadoes for any parameter with no constraint was the effective bulk shear range of 45 to 70 kt. For this reason, at least 50 kt of effective shear was added as a

218 constraint to show predictability for different parameters. It should be noted that this
219 constraint was also based upon values relevant to organized, severe convection in the
220 southeast U.S. The three parameters investigated in detail here are 0-1-km shear, 0-1-km SRH,
221 and MLLCL heights. These parameters showed the best predictability when the constraint of 50
222 kt of effective bulk shear was added.

223 As shown is Fig. 6a, predictability of tornado events for 0-1-km shear is better when the
224 constraint of at least 50 kt of effective shear was added. Specifically, strong low-level shear
225 regimes between 40 to 60 kt show the best predictability for this parameter. In addition, the
226 southeast U.S. shows better predictability than everywhere else and these distributions are
227 statistical significantly different which demonstrates that the southeast U.S. does follow a high-
228 shear regime for tornado environments. In addition to 0-1-km shear, 0-1-km SRH exhibits good
229 predictability; specifically, from 0 to 600 ($m^2 s^{-2}$) when at least 50 kt of effective shear is added
230 as a constraint. Although the southeast U.S offers better predictability than the remainder of
231 the CONUS after 200 ($m^2 s^{-2}$), the distributions are only statistically significantly different for the
232 parameter range of 400-600 ($m^2 s^{-2}$) as shown in Fig. 6b.

233 The last variable associated with better predictability compared to the rest of the
234 CONUS when 50 kt of effective shear is added as a constraint is MLLCL heights, particularly
235 when MLLCL heights are low (300-800 m) as depicted in Fig. 6c. Between this range, conditional
236 probabilities increase from 1% to about 11% and then begin to steadily decrease as the number
237 of environments also decreases. This trend in the southeast U.S. is consistent with the
238 remainder of the CONUS with regard to low probabilities as LCL heights reach 1000m. This is a
239 reflection that not many environments in the United States with high MLLCLs go on to produce

240 downstream tornadoes, even when there is strong, deep vertical shear in the background
241 environment.
242
243 c.) *Statistical results for the coastal region subset*
244 To illustrate predictability within the southeast U.S., the coastal region was added as a
245 subset to see how predictability would compare to everywhere else. Throughout this study, it
246 was found that when the coastal region subset was compared to the remainder of the CONUS,
247 the coastal region generally offered worse predictability than everywhere else. Conditional
248 probabilities of tornado events (weak or significant) for the coastal region subset are found to
249 increase with values of STP ranging from 0 to 5. Along with that, most of the tornado events
250 occur in this range and the distribution is statistically significantly different than the rest of the
251 CONUS. Although the coastal region subset offers good predictability for this STP range, the
252 remainder of the CONUS offers consistently better predictability, as shown in Fig. 7. As the
253 coastal region begins a decline in probabilities, the rest of the CONUS offers a continuous, steep
254 slope through STP values of 8.
255 Tornado events for the coastal region subset are found to vary slightly with effective
256 bulk shear as compared to the rest of the CONUS, only reaching a maximum probability of 6%
257 at 65 kt. We speculate this to be because the of the smaller sample size as shear magnitudes
258 increase. Furthermore, the coastal region subset offers worse predictability than everywhere
259 else between the range of 35-70 kt when the distributions become statistically significantly
260 different.
261

d.) Predictability differences based on tornado intensity variations

Predictability for weak tornadoes (EF0-EF1) and significant tornadoes (EF2-EF5) can be distinguished for different parameters. When 50 kt of effective bulk shear is added as a constraint to 0-1-km SRH, the increase in conditional probabilities for significant tornadoes is much greater than weak tornadoes as shown in Fig. 8a and 8b. As shown in Fig. 8b and 8c, large magnitudes of vertical shear, in relationship with downstream tornado occurrence highlighting 0-1-km shear of 60 kt, 13% and 6% of those grid boxes verify with weak and significant tornadoes, respectively. Furthermore, sizeable magnitudes of effective SRH for weak and significant tornadoes occur within 0 to 350 (m^2 s^{-2}) as shown in Fig. 8e and 8f, respectively; however, the relationship with downstream tornado occurrence emphasizing effective SRH of 550 (m^2 s^{-2}), 8% and 13% of those grid boxes verify with weak and significant tornadoes, respectively.

Conclusions

The Statistical Severe Convective Risk Assessment Model (Hart and Cohen 2016a) helped show the relationship of predictability between the southeast U.S. and everywhere else, which is a mutually exclusive area outside of the general southeast United States across the contiguous United States, and the coastal region subset and the remainder of the CONUS was investigated in this present study. Various parameters, with constraints, showed an increase in conditional probabilities and overall better predictability for the southeast U.S. than the rest of the CONUS. Specifically, at least 50 kt of effective bulk shear is found to offer better predictability for the southeast U.S. than everywhere else when added as a constraint for

different parameters. The coastal region subset, in general, offered worse predictability than everywhere else when the distributions became statistically significantly different. This illustrates the difficulty predicting nocturnal tornadoes in the coastal region subset during the period from November to May. In addition, tornado intensity was considered for different parameters and revealed that for strong low-level shear with deep shear, weak tornadoes offer better predictability than significant tornadoes in the southeast U.S. Ultimately, this work can directly influence the warn-on-forecast initiative to help improve lead times for high-impact events based on parameters and a lightning-producing thunderstorm.

Acknowledgments

The author would like to extend gratitude to Dr. Daphne LaDue (OU CAPS) and Briana Lynch for putting on an exceptional summer for all of the REU students. Additionally, thanks are extended to Andrew Moore for all of the coding help and advice throughout the summer. Finally, the author would like to thank David Nowicki for his contributions to this project and continued capacity as a productive and determined research partner. This work was prepared by the authors with funding was provided by the National Science Foundation Grant No. AGS-1560419, and NOAA/Office of Oceanic and Atmospheric Research under NOAA-University of Oklahoma Cooperative Agreement #NA11OAR4320072, U.S. Department of Commerce. The statements, findings, conclusions, and recommendations are those of the author(s) and do not necessarily reflect the views of the National Science Foundation, NOAA, or the U.S. Department of Commerce.

306 **References**

307 Ashley, W. S., Krmenec, A. J., & Schwantes, R. (2008). Vulnerability due to Nocturnal Tornadoes.
308 *Weather and Forecasting*, **23**, 795–807. doi:10.1175/2008waf2222132.1
309
310 Bothwell, P. D., J. A. Hart, and R. L. Thompson, 2002: An integrated three-dimensional objective
311 analysis scheme in use at the Storm Prediction Center. Preprints, *21st Conference on Severe*
312 *Local Storms*, San Antonio, TX, Amer. Meteor. Soc., J117–J120.
313
314 Bryan, G. H., J. C. Wyngaard, and J. M. Fritsch, 2003: Resolution requirements for the simulation
315 of deep moist convection. *Mon. Wea. Rev.*, **131**, 2394–2416.
316
317 Bunkers, M. J., B. A. Klimowski, J. W. Zeitler, R. L. Thompson, and M. L. Weisman, 2000:
318 Predicting supercell motion using a new hodograph technique. *Wea. Forecasting*, **15**, 61–79.
319
320 Burgess, D. W., and L. R. Lemon, 1990: Severe thunderstorm detection by radar. *Radar in*
321 *Meteorology.* D. Atlas, Ed., Amer. Meteor. Soc., 619–647.
322
323 Cohen, A. E., and Coauthors, (2015): A Review of Planetary Boundary Layer Parameterization
324 Schemes and Their Sensitivity in Simulating Southeastern U.S. Cold Season Severe Weather
325 Environments. *Weather and Forecasting*, **30**, 591-612. doi: 10.1175/WAF-D-00105.1
326

Doswell, C. A., III, and D. M. Schultz, 2006: On the use of indices and parameters in forecasting severe storms. *Electronic J. Severe Storms Meteor.*, **1**(3), 1–22.

Galway, J. O., 1992: Early severe thunderstorm forecasting and research by the United States Weather Bureau. *Wea. Forecasting*, **7**, 564–587.

____, and Pearson, A., (1981): Winter Tornado Outbreaks. *Monthly Weather Review*, **109**, 1072-1080.

Guyer, J. L., & Dean, D. R., (2010): Tornadoes Within Weak CAPE Environments Across the Continental United States. *25th Conference on Severe Local Storms*.

Guyer, J. G., and Imy, D. A., (2006): Cool Season Significant (F2-F5) Tornadoes in the Gulf Coast States. *23rd Conference on Severe Local Storms*.

Hart, J. A., & Cohen, A. E. (2016). The Statistical Severe Convective Risk Assessment Model. *Weather and Forecasting*, **31**, 1697–1714. doi:10.1175/waf-d-16-0004.1

____, & Cohen, A. E. (2016). The Challenge of Forecasting Significant Tornadoes from June to October Using Convective Parameters. *Weather and Forecasting*, **31**, 2075-2084. doi: 10.1175/WAF-D-16-005.1

Jankov, I., and W. A. Gallus Jr., 2004: MCS rainfall forecast accuracy as a function of large-scale forcing. *Wea. Forecasting*, **19**, 428–439.

Johns, R. H., and C. A. Doswell, 1992: Severe local storms forecasting. *Wea. Forecasting,* **7,** 588–612.

Kanji, G. K. (2006). *100 statistical tests*. London: Sage.

Lewis, J., 1989: Realtime lightning data and its application in forecasting convective activity. Preprints, *12th Conf. Wea. Analysis and Forecasting,* Monterey, CA, Amer. Meteor. Soc., 97–102.

Nowicki, D. P., cited 2017: How forecasters anticipate nocturnal, cool-season southeastern tornado events. [Available online at http://www.caps.ou.edu/reu/reu17/finalpapers/Nowicki-Paper.pdf.]

Scofield, R. A., and J. F. W. Purdom, 1986: The use of satellite data for mesoscale analyses and forecasting applications. *Mesoscale Meteorology and Forecasting,* P. S. Ray, Ed., Amer. Meteor. Soc., 118–150.

Schwartz, C. S., G. S. Romine, K. R. Smith, and M. L. Weisman, 2014: Characterizing and Optimizing Precipitation Forecasts from a Convection-Permitting Ensemble Initialized by a Mesoscale Ensemble Kalman Filter. *Wea. Forecasting*, **29**, 1295–1318.

Thompson, R. L., C. M. Mead, and R. Edwards, 2007: Effective storm-relative helicity and bulk shear in supercell thunderstorm environments. *Wea. Forecasting*, **22**, 102–115.

——, B. T. Smith, J. S. Grams, A. R. Dean, and C. Broyles, 2012: Convective Modes for Significant Severe Thunderstorms in the Contiguous United States. Part II: Supercell and QLCS Tornado Environments. *Wea. Forecasting*, **27**, 1136–1154.

U.S. Tornado Climatology. *National Climatic Data Center*. https://www.ncdc.noaa.gov/climate-information/extreme-events/us-tornado-climatology. Accessed 26 July 2017

Figure Captions

FIG. 1. Example of climatology of tornadoes by state from 1991-2010 for (a) November (b) December (c) January (d) February (e) March (f) April (g) March (National Climate Data Center 2017).

FIG. 2. Map of study domains. Within the red-shaded domain represents the general southeast and within the blue-shaded domain represents the coastal region subset of the general southeast.

391

392 FIG. 3. Example of annual average tornado watches per year (20y Avg. 1993-2012) with watches
393 per county shown.

394

395 FIG. 4. SSCRAM conditional probability output (Hart and Cohen 2016) at 15Z based on
396 significant tornado parameter, 100-mb mixed-layer CAPE, 3-km AGL wind speed, and season.
397 Red-highlighted grid boxes indicate at least one CG lightning strike within that grid box.
398 Conditional probabilities are shown within each grid box.

399

400 FIG. 5. (a) Conditional probability plot for the southeast U.S. (red) with p-values plotted (green
401 or yellow) overlaid corresponding to respective ranges, coastal region subset (blue) with p-
402 values overlaid on respective ranges, and everywhere else (black) for 0-1-km shear (kt) on the
403 x-axis, table of total environments relative to each distribution below the x-axis, and conditional
404 probability on the y-axis. (b) As in Fig. 5a, but for 0-1-km SRH. (c) as in Fig. 5a, but for MLCAPE.
405 (d) As in Fig. 5a, but for MLLCL height. (e) As in Fig. 5a, but for effective bulk shear. (f) As in Fig.
406 5a, but for effective SRH. (f) As in Fig. 5a, but for STP.

407

408 FIG. 6. (a) As in Fig. 5a, but with a constraint of 50 kt of effective bulk shear for 0-1-km shear.
409 (b) As in Fig. 6a, but for 0-1-km SRH. (6) As in Fig. 6a, but for 0-1-km MLLCL height.

410

411 FIG. 7. As in Fig. 5a, but for STP.

412

413 FIG. 8. As in Fig. 6a, but for weak tornadoes for 0-1-km SRH. (b) As in Fig. 6b, but for significant

414 tornadoes. (c) As in Fig. 8a, but for 0-1-km shear. (d) As in Fig. 8b, but for 0-1-km shear. (e) As in

415 Fig. 8a, but for effective SRH. (f) As in Fig. 8b, but for effective SRH.

416

417 **Figures**

418 (1)

419 (a)

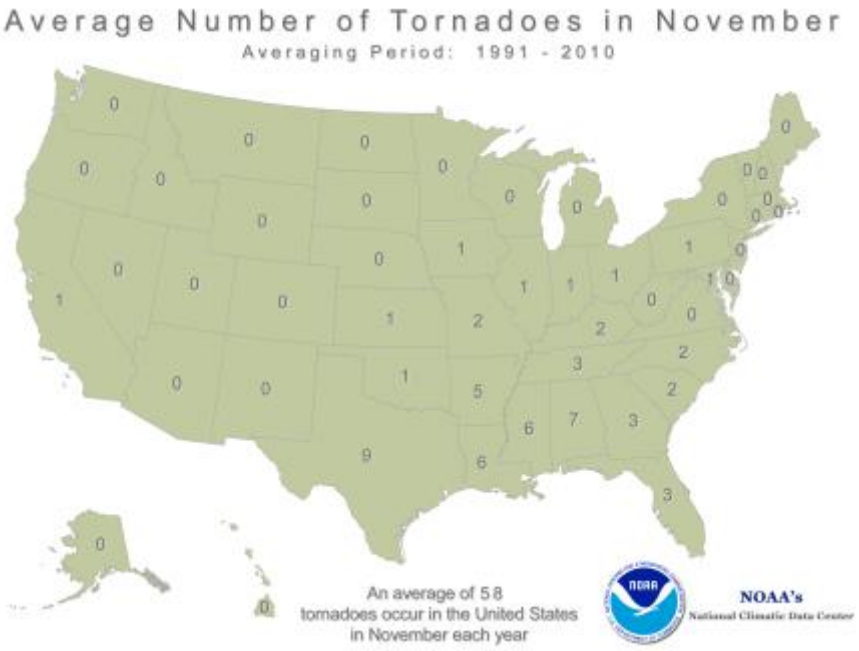

420

421

422 (b)

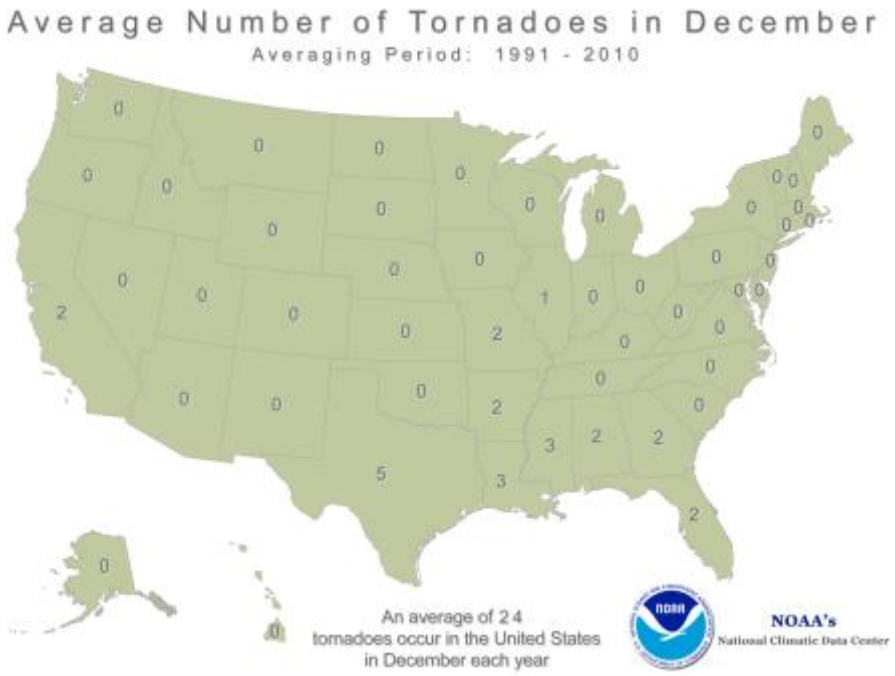
Average Number of Tornadoes in December
Averaging Period: 1991 - 2010
An average of 24
tornadoes occur in the United States
in December each year
NOAA's
National Climatic Data Center

(c)

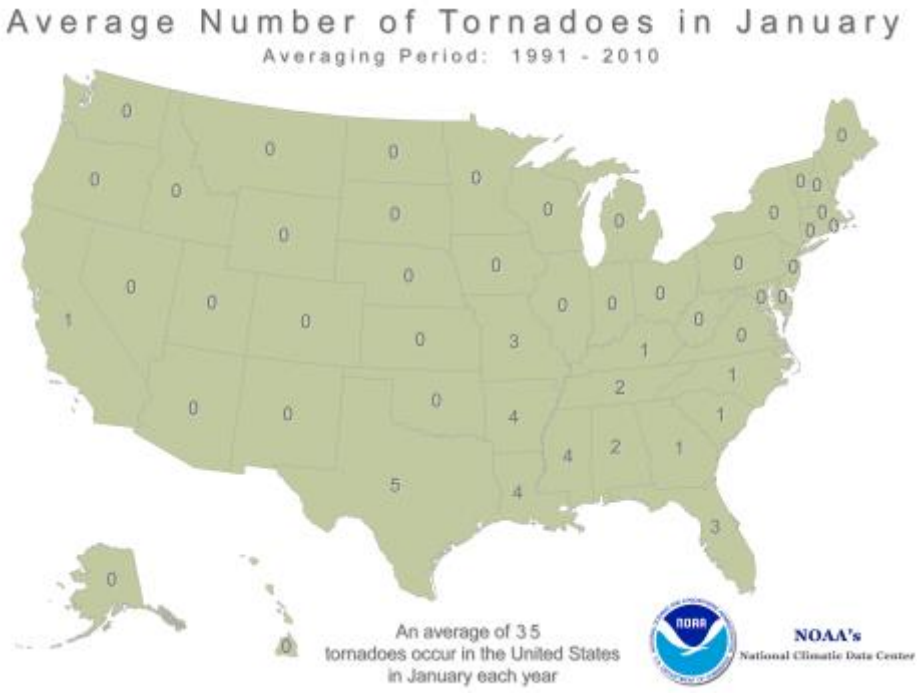
Average Number of Tornadoes in January
Averaging Period: 1991 - 2010
An average of 35
tornadoes occur in the United States
in January each year
NOAA's
National Climatic Data Center

(d)

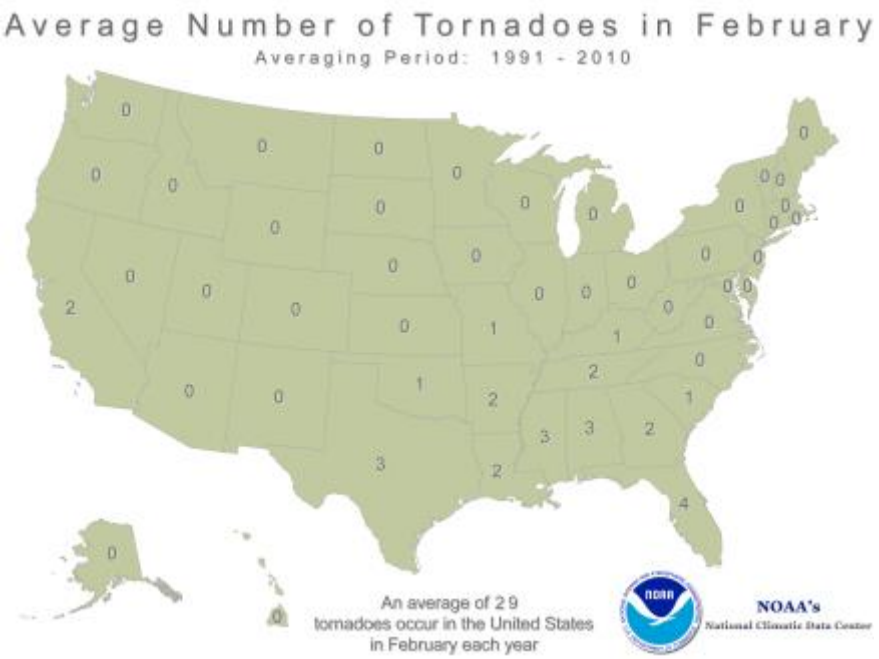
Average Number of Tornadoes in February
Averaging Period: 1991 - 2010
An average of 2.9
tornadoes occur in the United States
in February each year
NOAA's
National Climatic Data Center

(e)

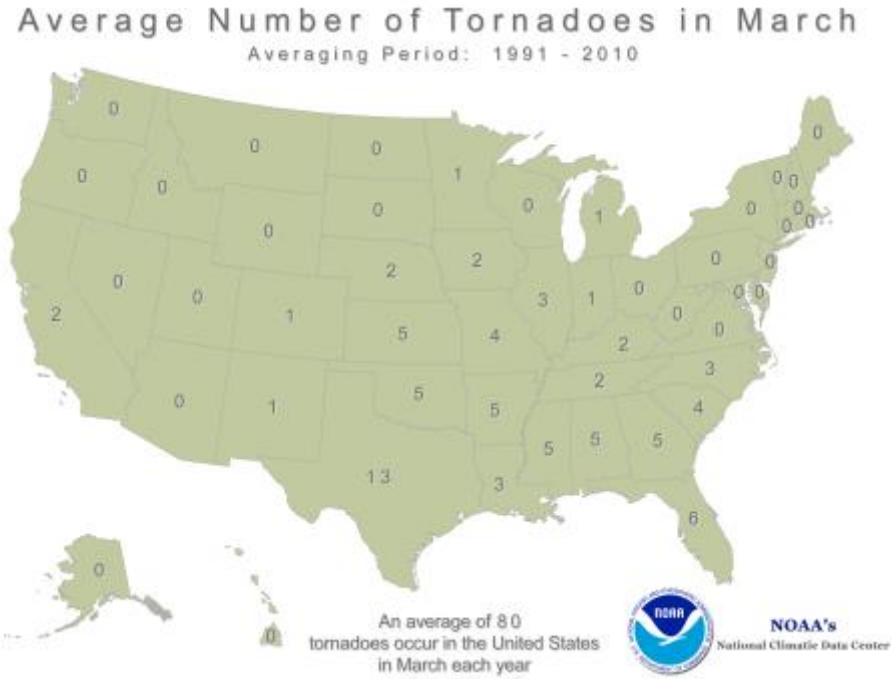
Average Number of Tornadoes in March
Averaging Period: 1991 - 2010
An average of 8.0
tornadoes occur in the United States
in March each year
NOAA's
National Climatic Data Center

434

(f)

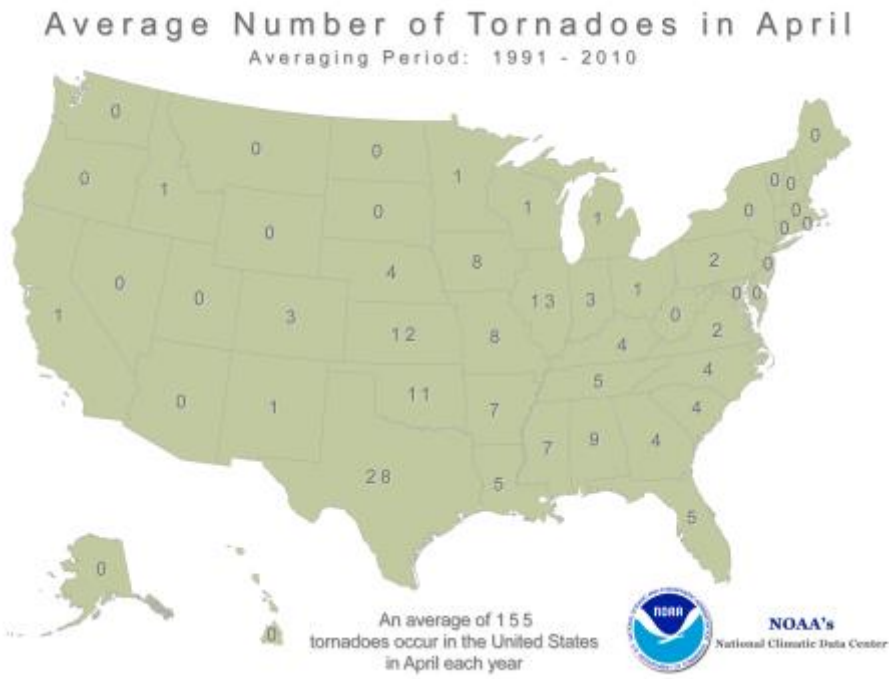

435

436

(g)

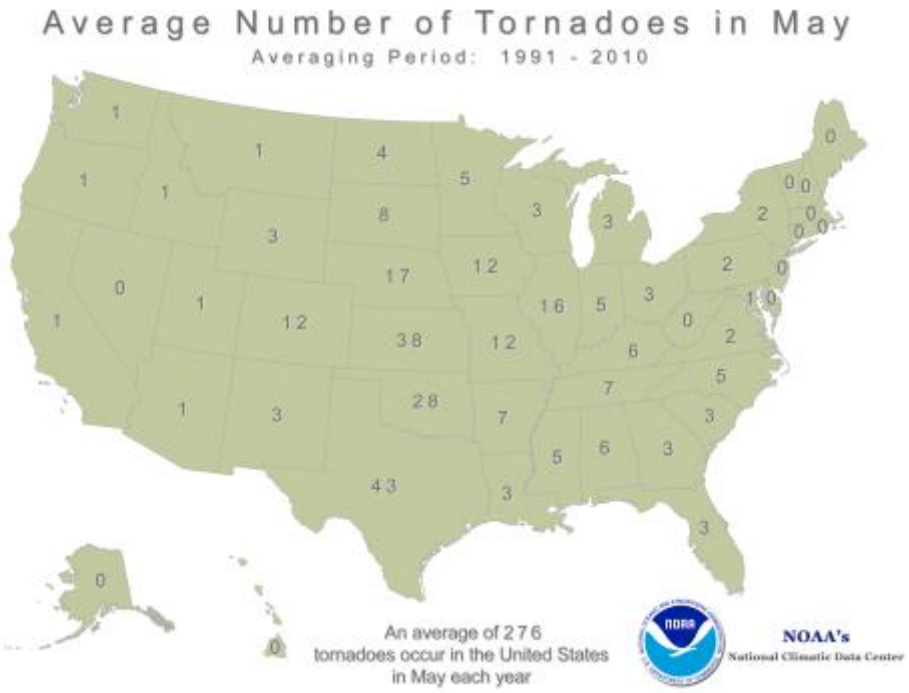

437

438 FIG. 1. Example of climatology of tornadoes by state from 1991-2010 for (a) November (b)

439 December (c) January (d) February (e) March (f) April (g) March (National Climate Data Center

440 2017).

441 (2)

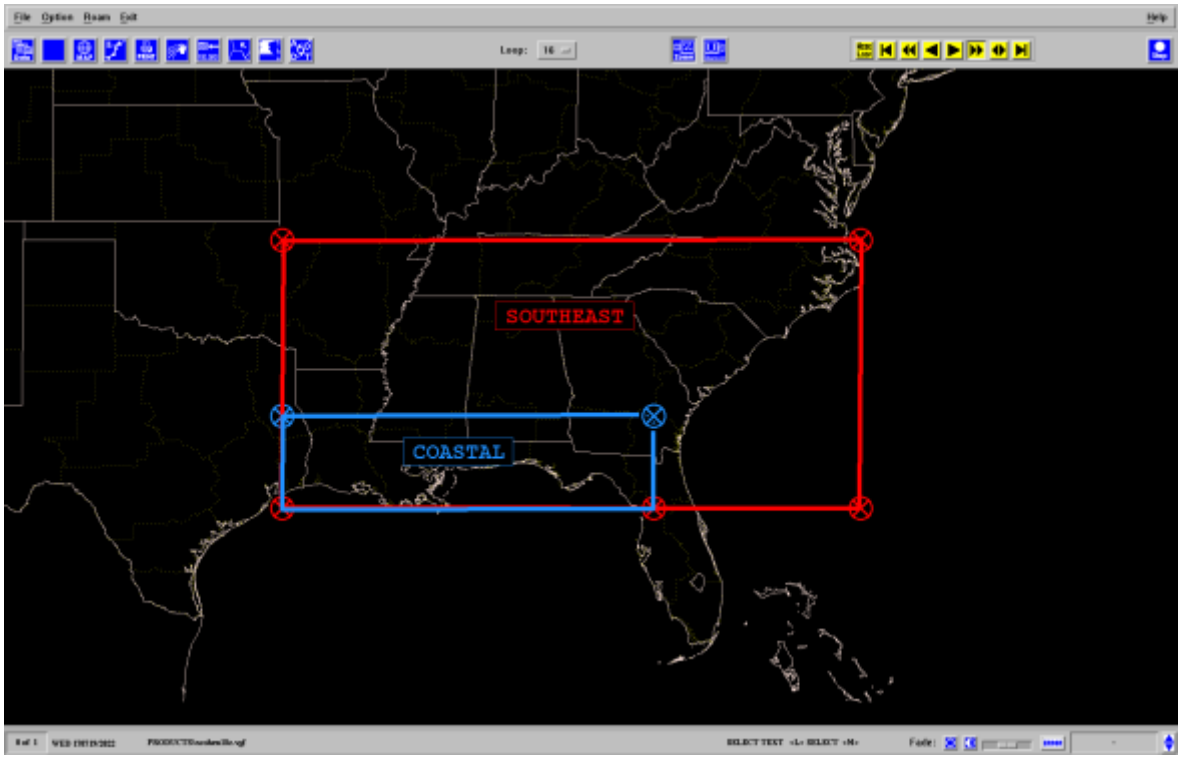

442

443 FIG. 2. Map of study domains. Within the red-shaded domain represents the general southeast

444 and within the blue-shaded domain represents the coastal region subset of the general

445 southeast.

446

447 (3)

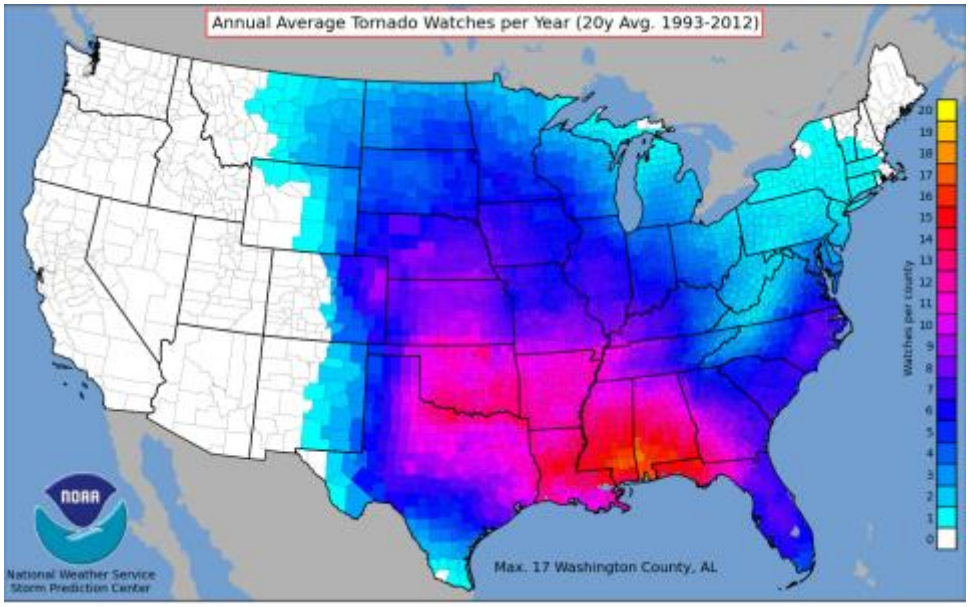

448

449 FIG. 3. Example of annual average tornado watches per year (20y Avg. 1993-2012) with watches

450 per county shown.

451

452 (4)

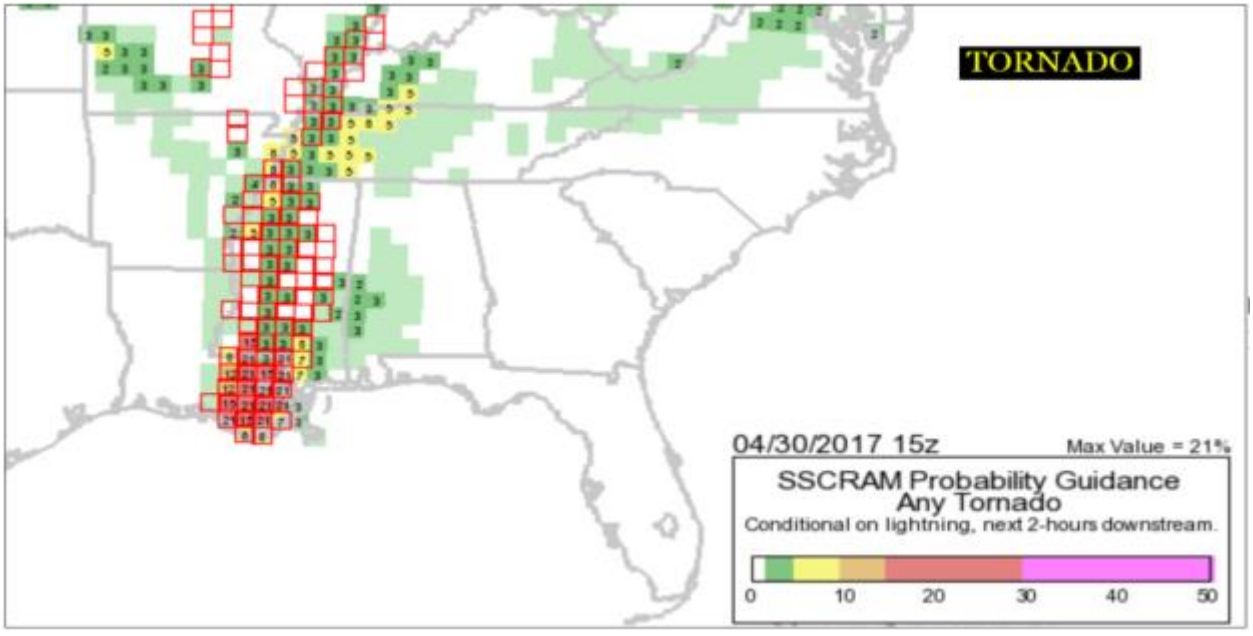

453

454 FIG. 4. SSCRAM conditional probability output (Hart and Cohen 2016) at 15Z based on

455 significant tornado parameter, 100-mb mixed-layer CAPE, 3-km AGL wind speed, and season.

456 Red-highlighted grid boxes indicate at least one CG lightning strike within that grid box.

457 Conditional probabilities are shown within each grid box.

458

459 (5)

460 (a)

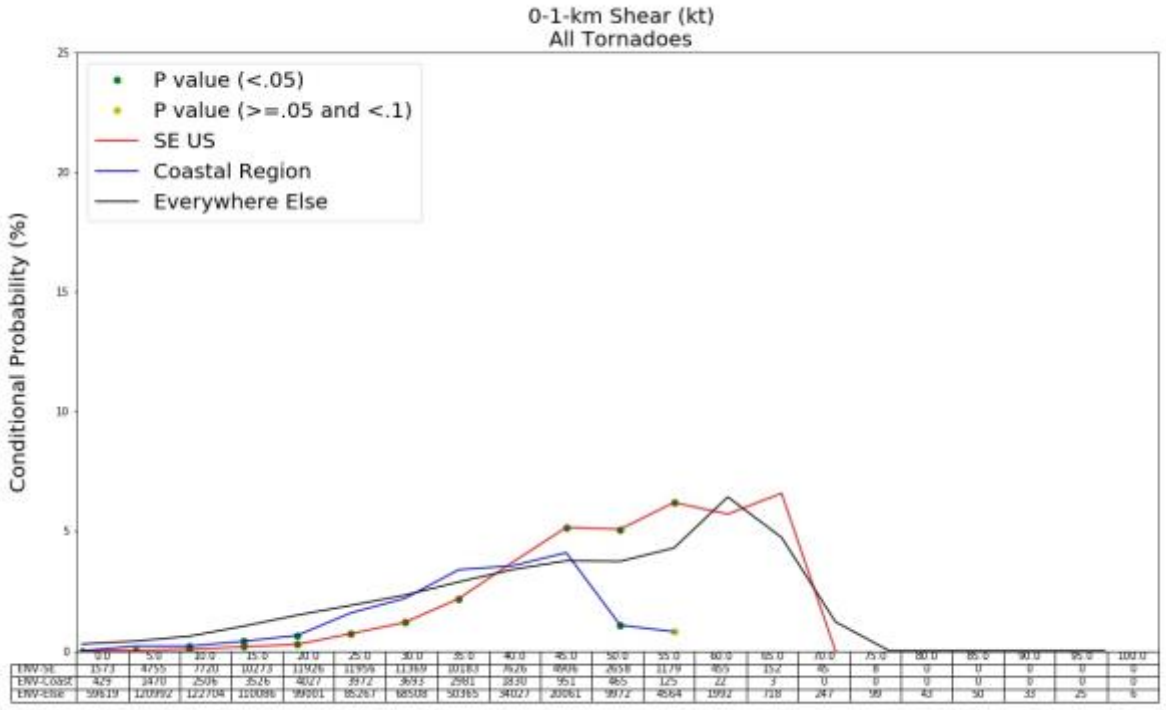

461

462

463

464

465

(b)

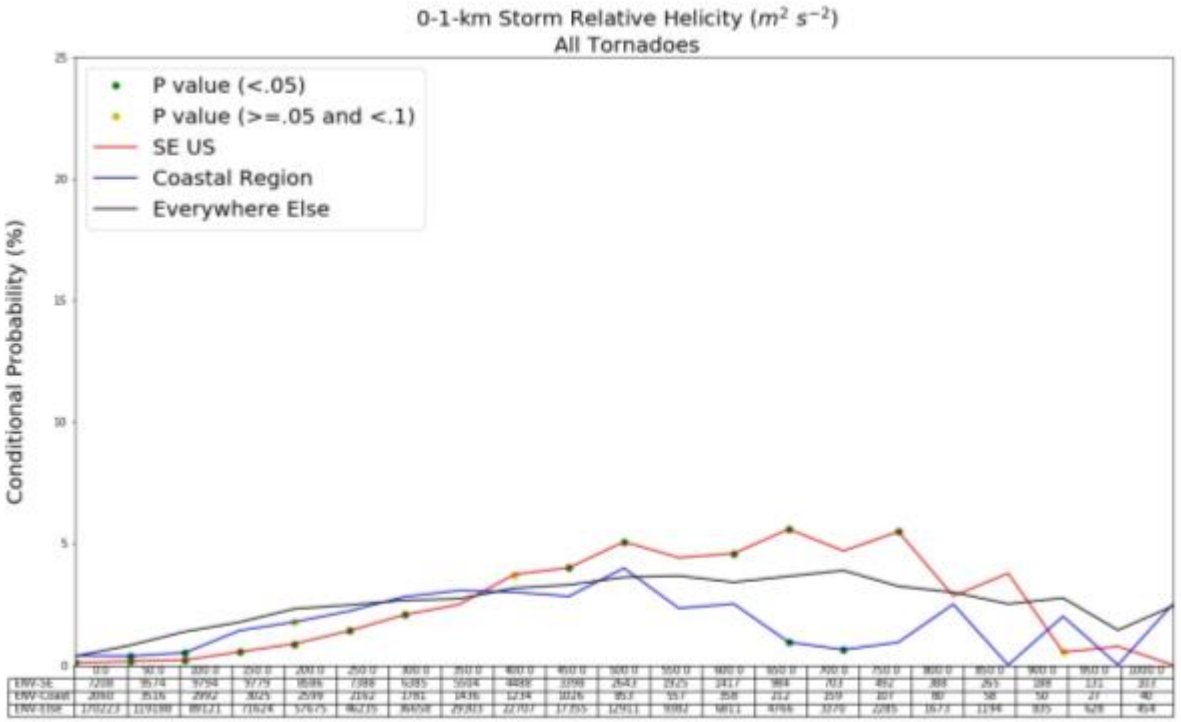
0-1-km Storm Relative Helicity (m^2 s^{-2})
All Tornadoes
P value (<.05)
P value (>=.05 and <.1)
SE US
Coastal Region
Everywhere Else
Conditional Probability (%)

(c)

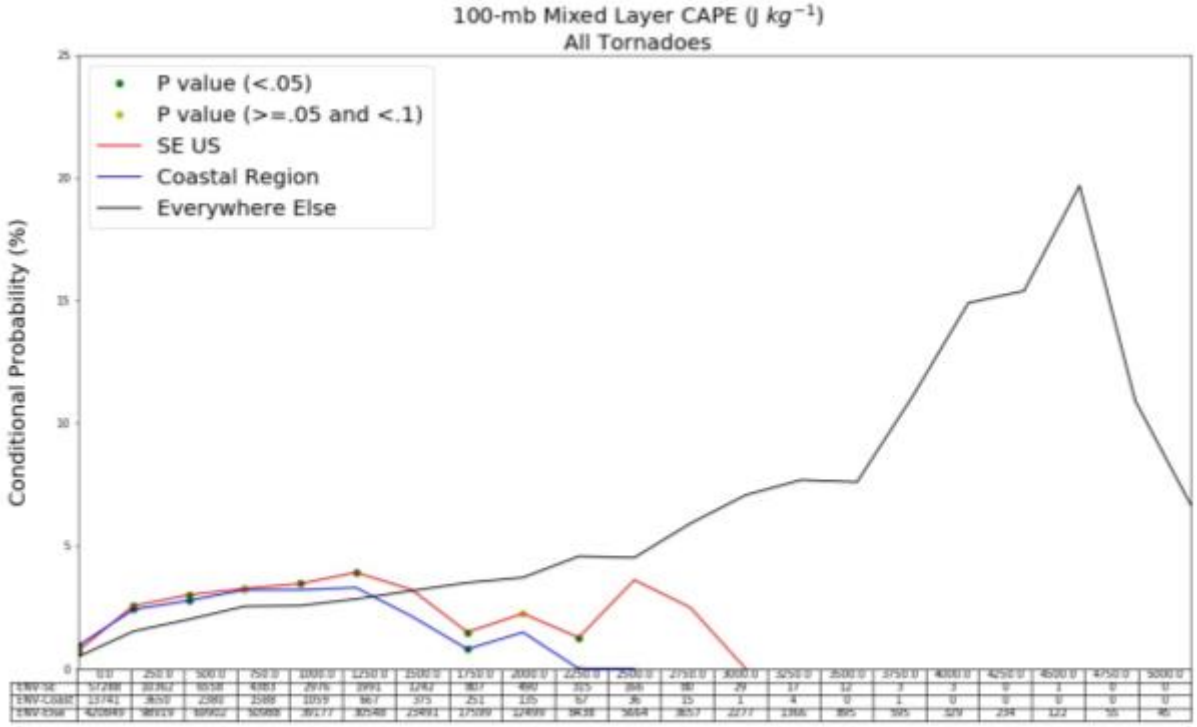
100-mb Mixed Layer CAPE (J kg^{-1})
All Tornadoes
P value (<.05)
P value (>=.05 and <.1)
SE US
Coastal Region
Everywhere Else
Conditional Probability (%)

(d)

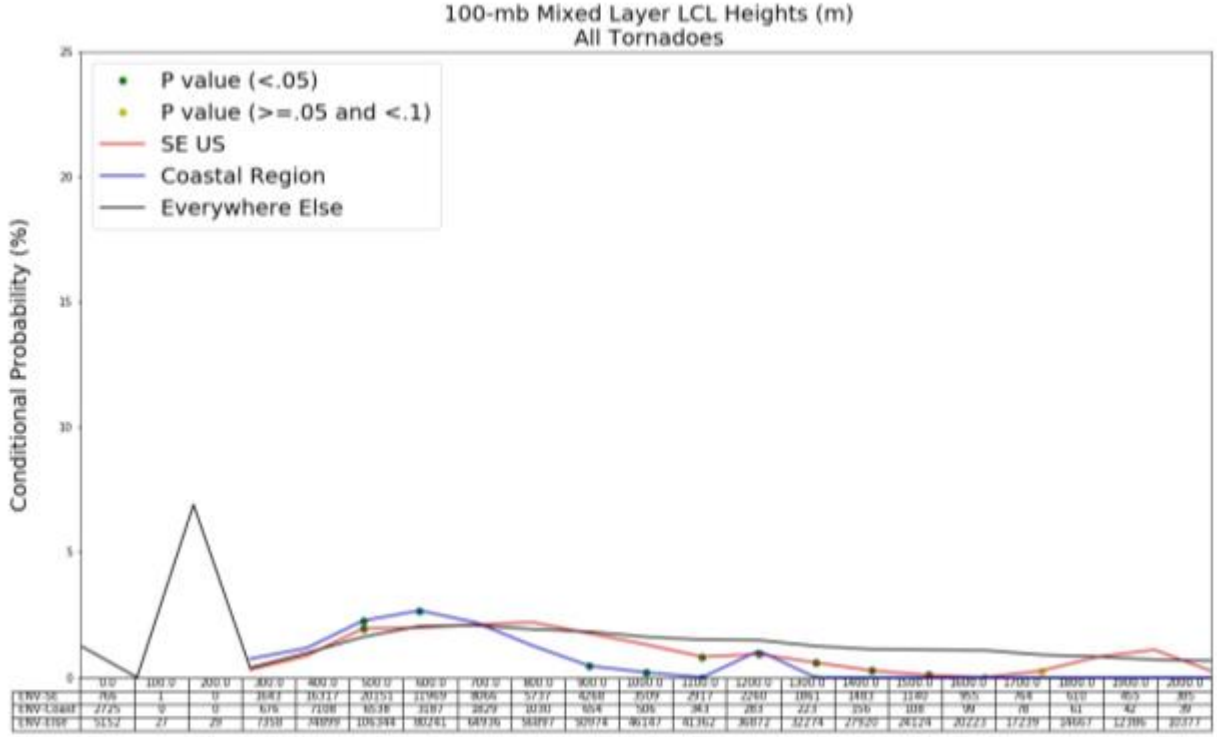
100-mb Mixed Layer LCL Heights (m)
All Tornadoes
P value (<.05)
P value (>=.05 and <.1)
SE US
Coastal Region
Everywhere Else
Conditional Probability (%)

(e)

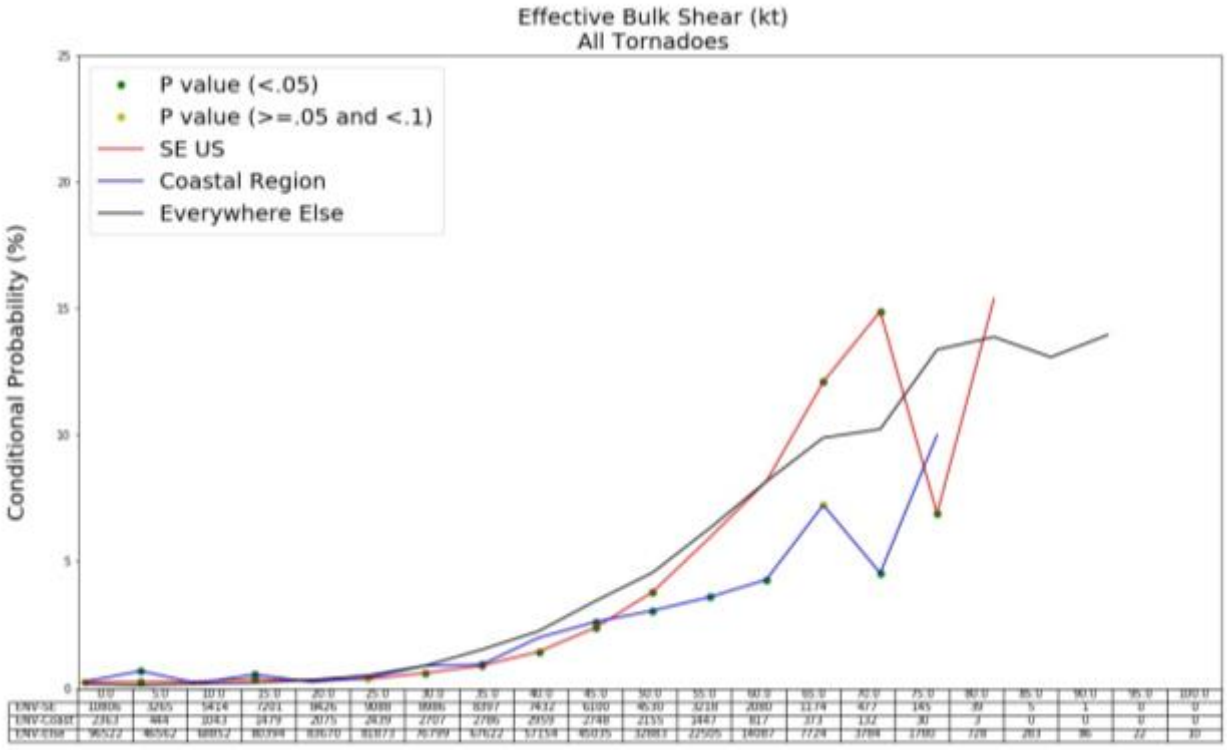
Effective Bulk Shear (kt)
All Tornadoes
P value (<.05)
P value (>=.05 and <.1)
SE US
Coastal Region
Everywhere Else
Conditional Probability (%)

473

(f)

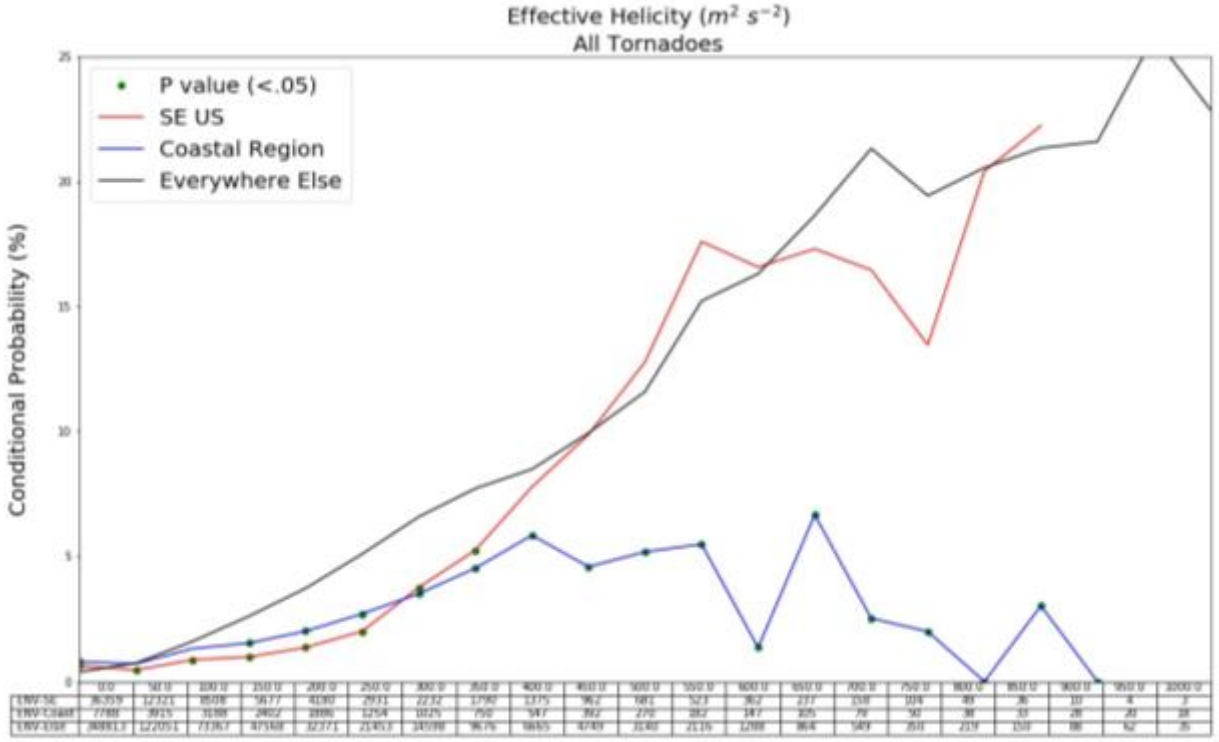

474

475

(g)

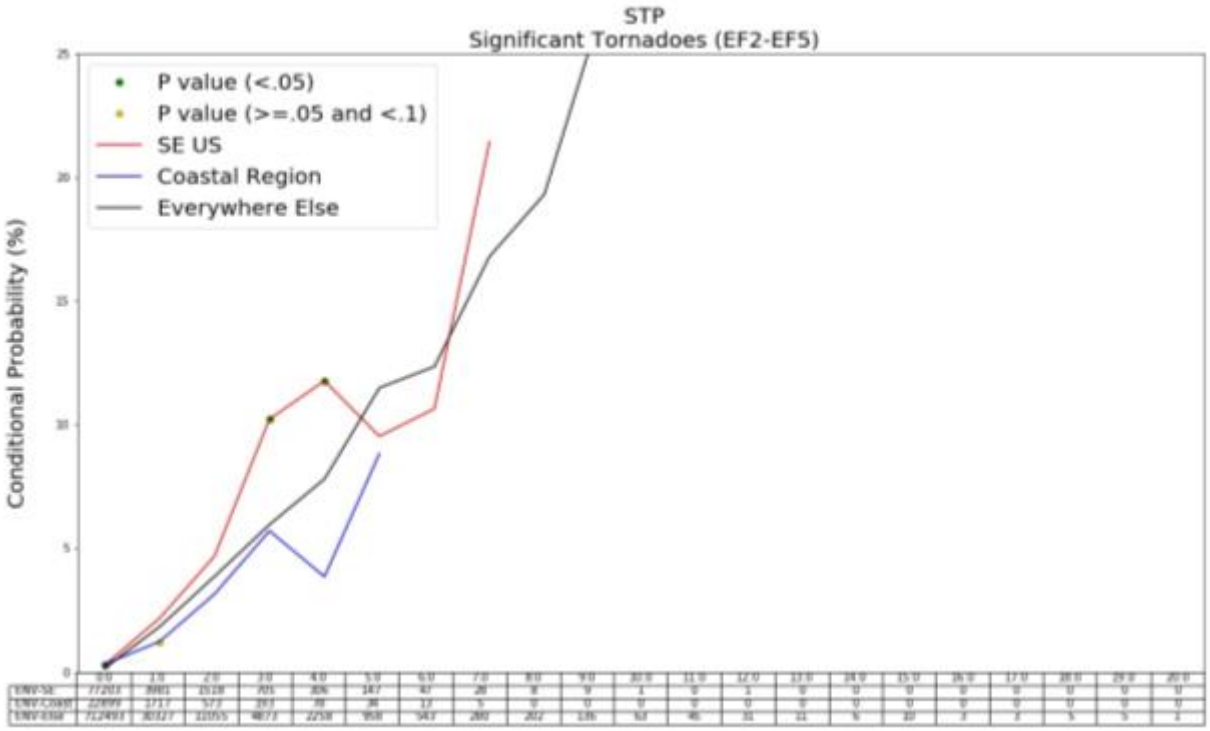

FIG. 5. (a) Conditional probability plot for the southeast U.S. (red) with p-values plotted (green or yellow) overlaid corresponding to respective ranges, coastal region subset (blue) with p-values overlaid on respective ranges, and everywhere else (black) for 0-1-km shear (kt) on the x-axis, table of total environments relative to each distribution below the x-axis, and conditional probability on the y-axis. (b) As in Fig. 5a, but for 0-1-km SRH. (c) as in Fig. 5a, but for MLCAPE. (d) As in Fig. 5a, but for MLLCL height. (e) As in Fig. 5a, but for effective bulk shear. (f) As in Fig. 5a, but for effective SRH. (f) As in Fig. 5a, but for STP.

(6)

(a)

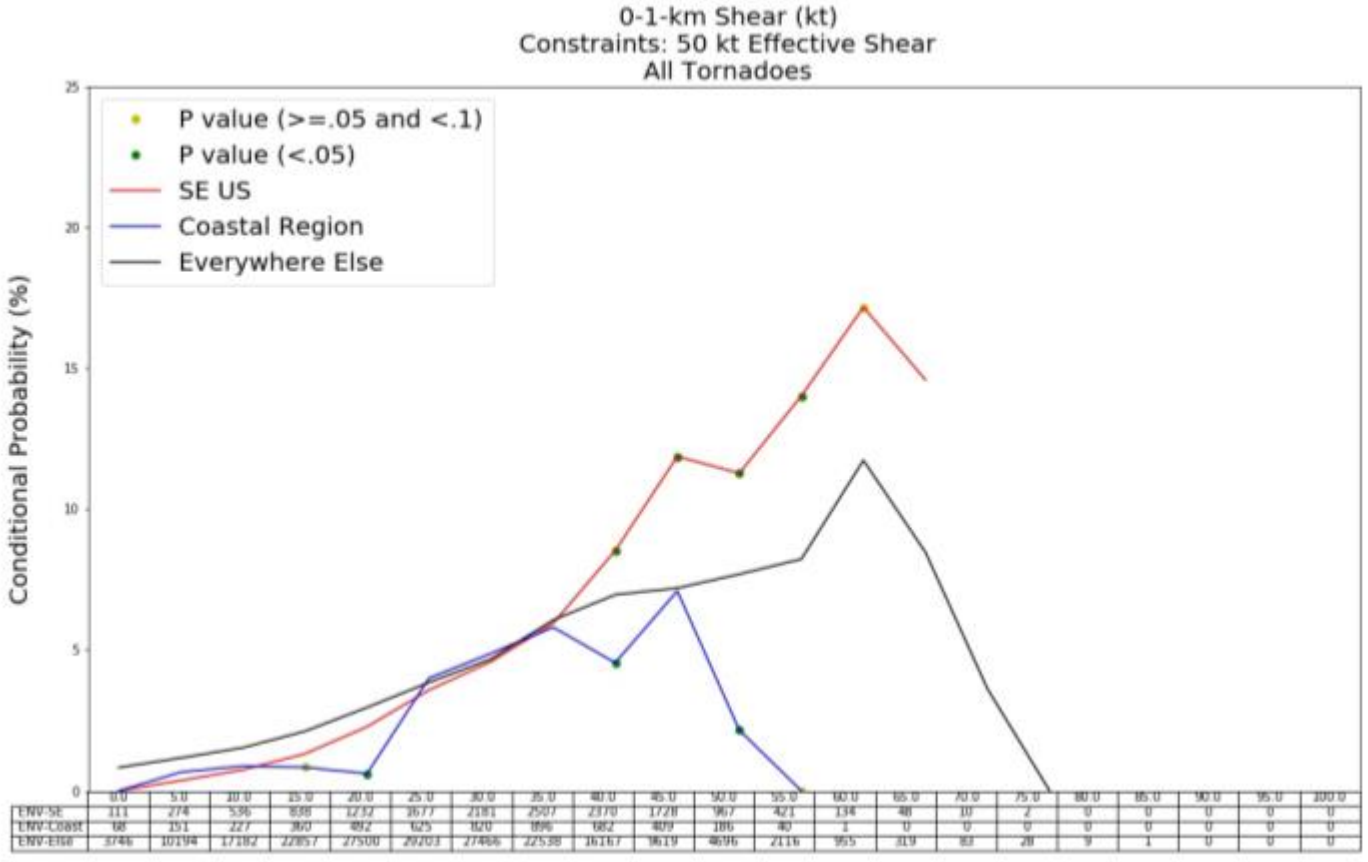

486

(b)

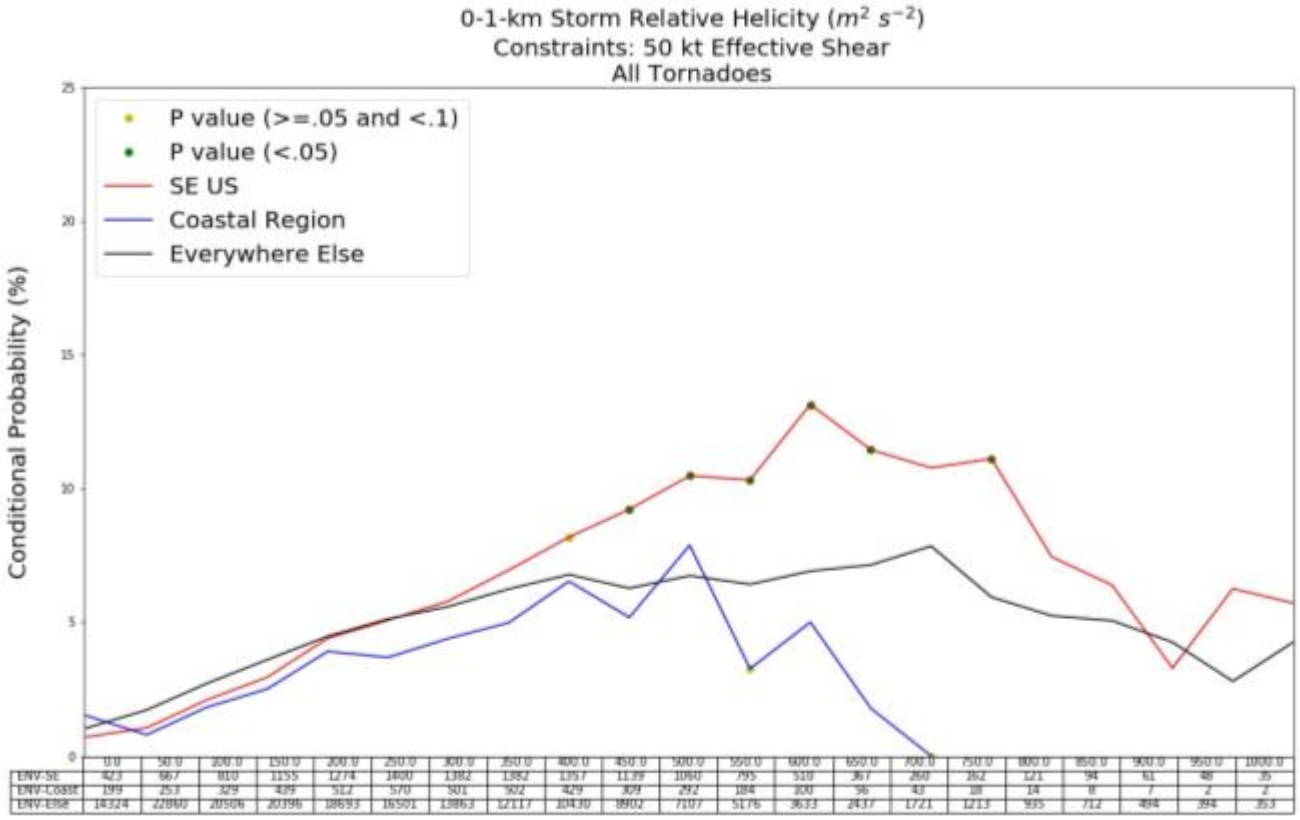

	0.0	50.0	100.0	150.0	200.0	250.0	300.0	350.0	400.0	450.0	500.0	550.0	600.0	650.0	700.0	750.0	800.0	850.0	900.0	950.0	1000.0
ENV-SE	423	667	810	1155	1274	1400	1382	1382	1357	1139	1060	795	510	367	260	162	121	94	61	48	35
ENV-Coast	199	253	329	439	512	570	501	502	429	309	292	184	100	56	43	18	14	8	7	2	2
ENV-Else	14324	22860	20506	20396	18693	16501	13863	12117	10430	8902	7107	5176	3633	2437	1721	1213	935	712	494	394	353

(c)

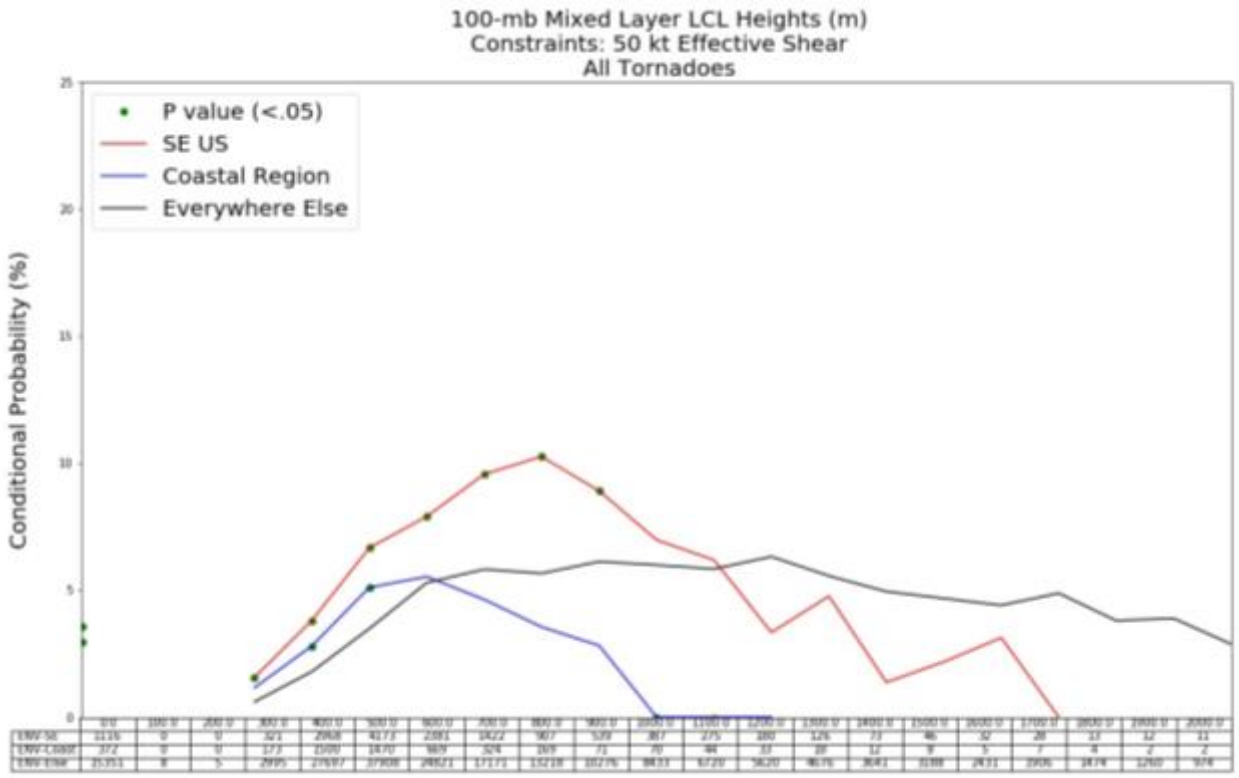

FIG. 6. (a) As in Fig. 5a, but with a constraint of 50 kt of effective bulk shear for 0-1-km shear. (b) As in Fig. 6a, but for 0-1-km SRH. (6) As in Fig. 6a, but for 0-1-km MLLCL height.

(7)

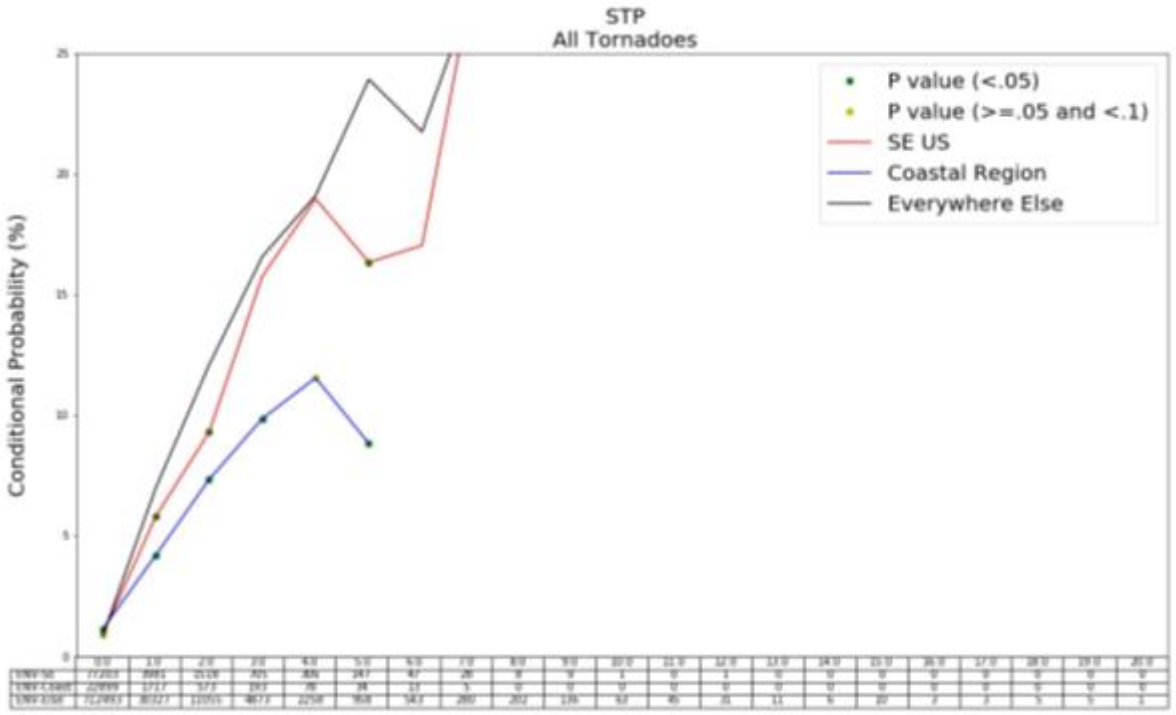

FIG. 7. As in Fig. 5a, but for STP.

(8)

(a)

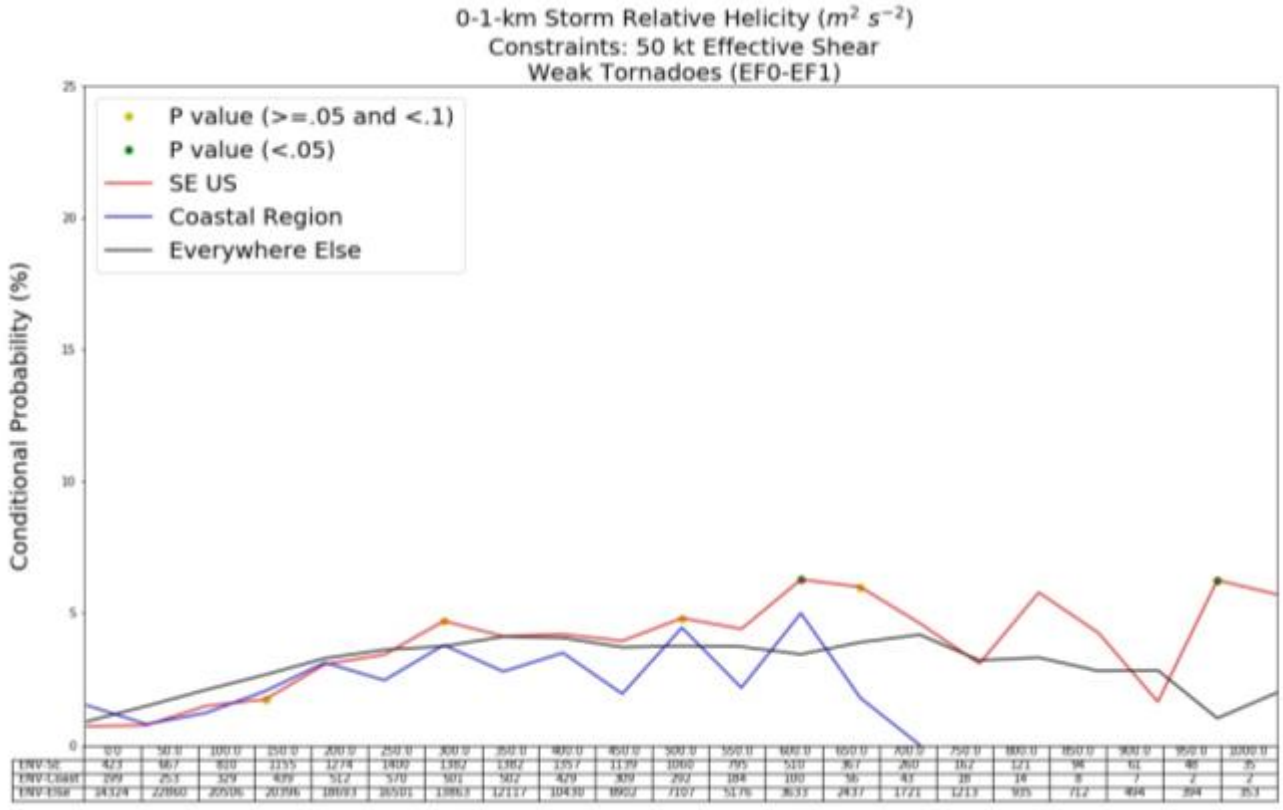

Bunker et al. p.33

524

(b)

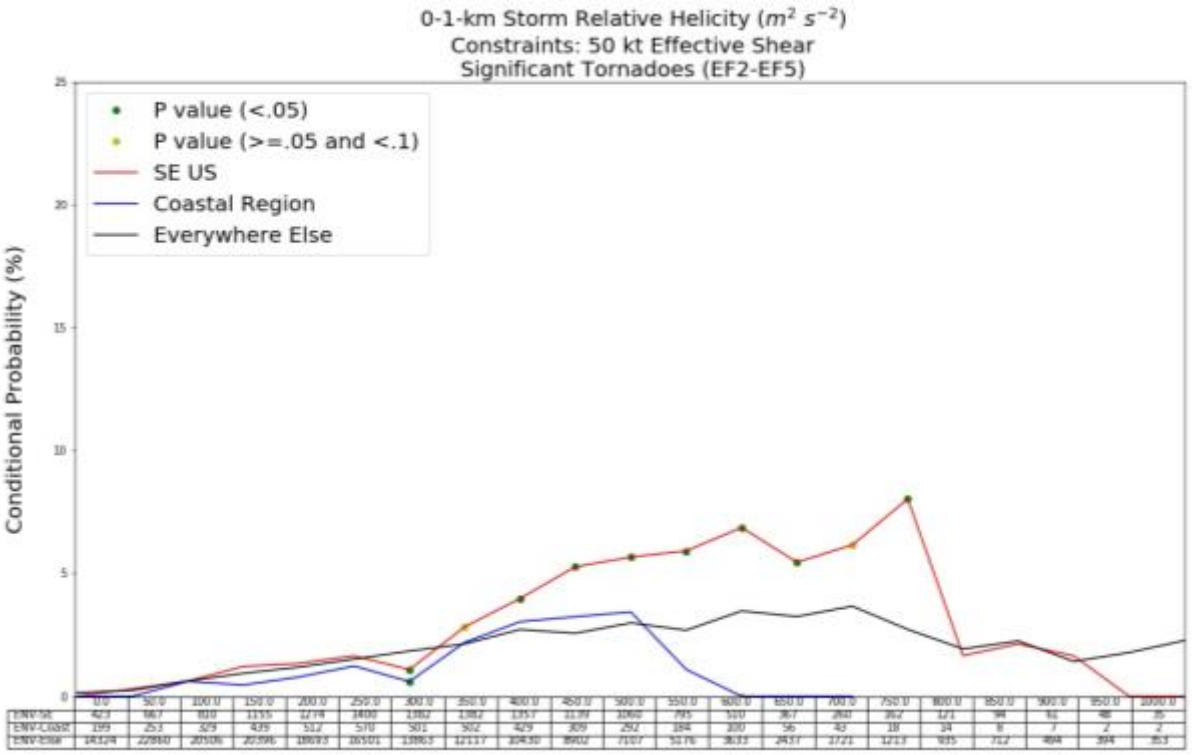

525

526

(c)

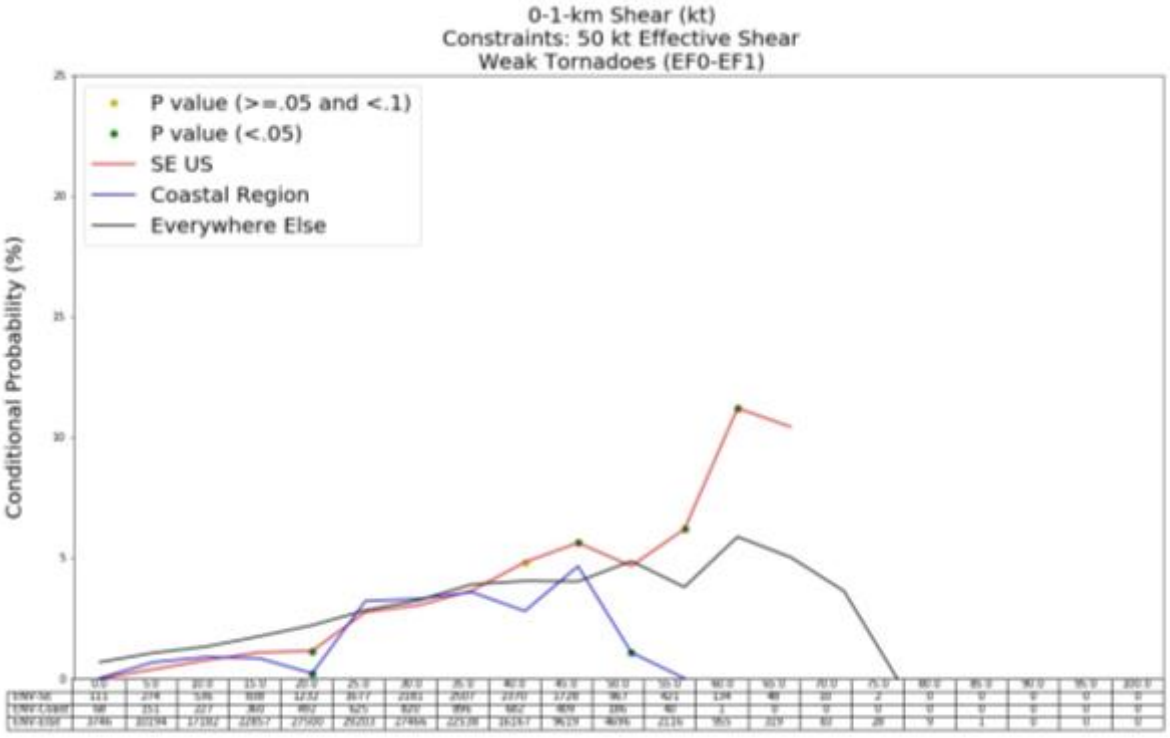

527

528 (d)

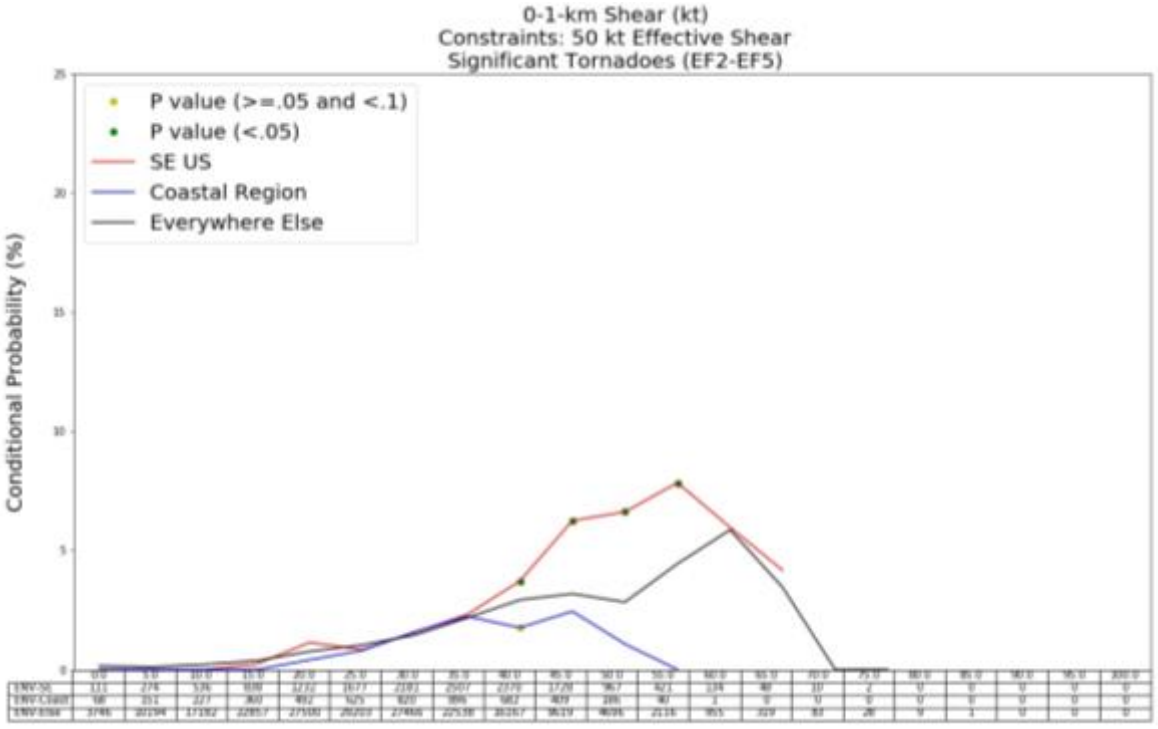

529

530 (e)

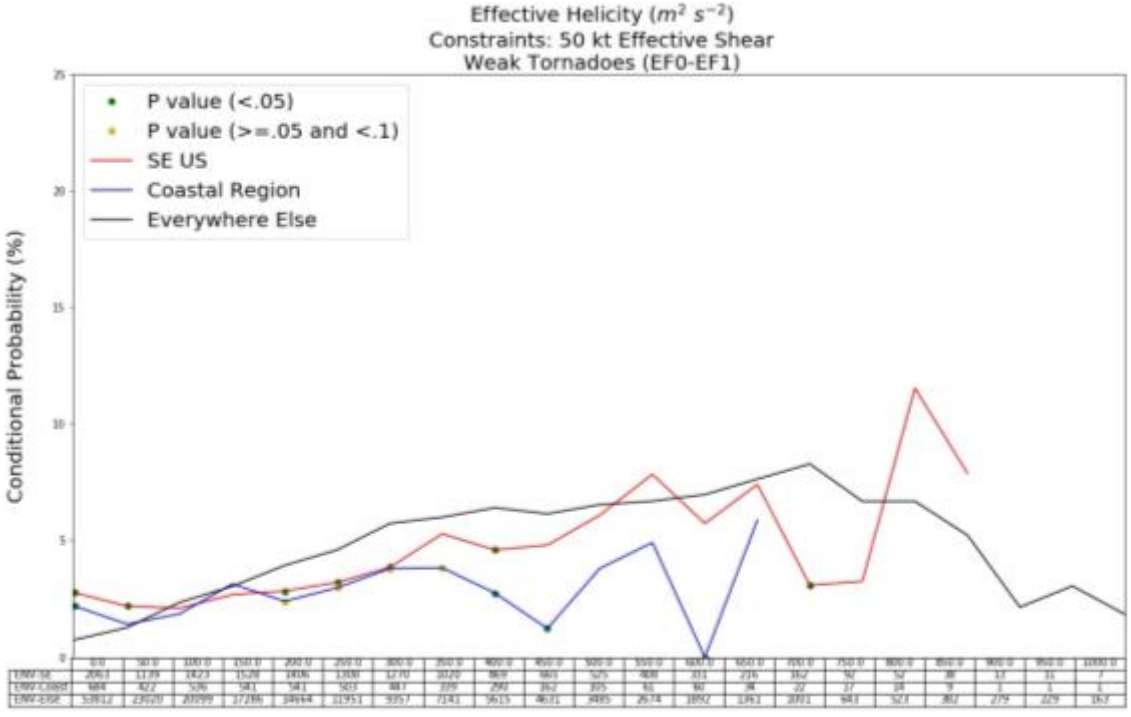

531

532 (f)

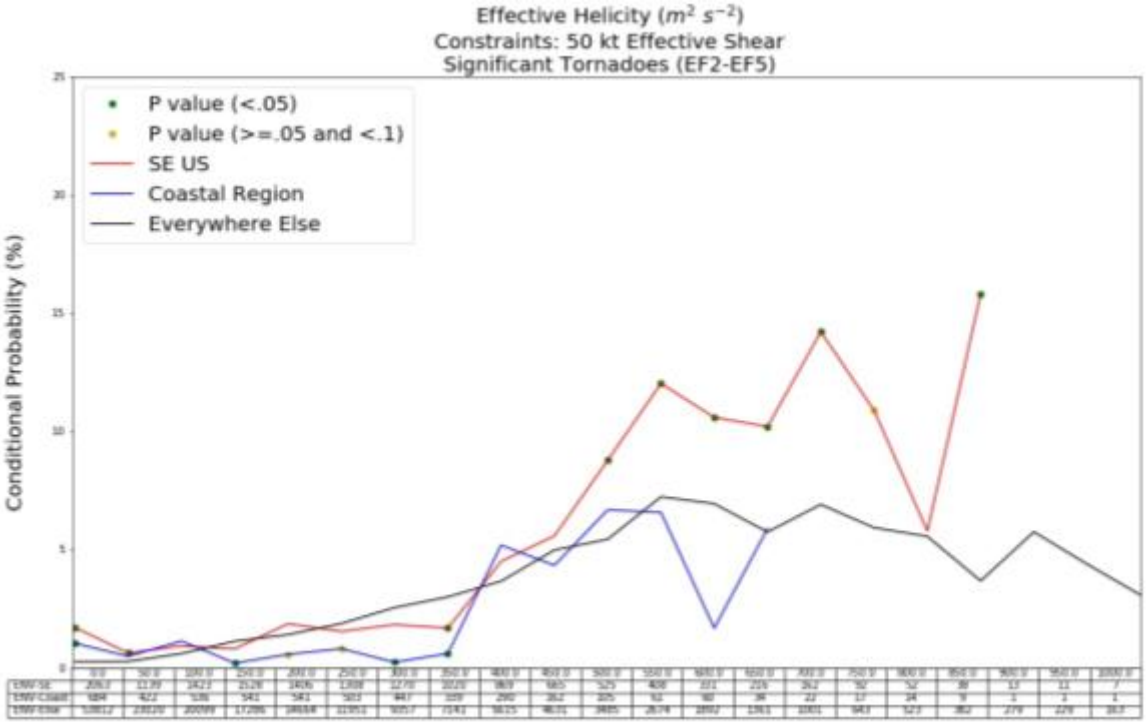

533

534 FIG. 8. As in Fig. 6a, but for weak tornadoes for 0-1-km SRH. (b) As in Fig. 6b, but for significant

535 tornadoes. (c) As in Fig. 8a, but for 0-1-km shear. (d) As in Fig. 8b, but for 0-1-km shear. (e) As in

536 Fig. 8a, but for effective SRH. (f) As in Fig. 8b, but for effective SRH.